

Non-magnetic and magnetic thiolate-protected Au₂₅ superatoms on Cu(111), Ag(111) and Au(111) surfaces

Xi Chen,¹ Mikkel Strange*,¹ and Hannu Häkkinen**^{1,2}

¹*Department of Chemistry, Nanoscience Center, University of Jyväskylä, 40014 Jyväskylä, Finland*

²*Department of Physics, Nanoscience Center, University of Jyväskylä, 40014 Jyväskylä, Finland*

(Dated: November 5, 2018)

Geometry, electronic structure, and magnetic properties of methylthiolate-stabilized Au₂₅L₁₈ and MnAu₂₄L₁₈ (L = SCH₃) clusters adsorbed on noble-metal (111) surfaces have been investigated by using spin-polarized density functional theory computations. The interaction between the cluster and the surface is found to be mediated by charge transfer mainly from or into the ligand monolayer. The electronic properties of the 13-atom metal core remain in all cases rather undisturbed as compared to the isolated clusters in gas phase. The Au₂₅L₁₈ cluster retains a clear HOMO - LUMO energy gap in the range of 0.7 eV to 1.0 eV depending on the surface. The ligand layer is able to decouple the electronic structure of the magnetic MnAu₂₄L₁₈ cluster from Au(111) surface, retaining a high local spin moment of close to 5 μ_B arising from the spin-polarized Mn(3d) electrons. These computations imply that the thiolate monolayer-protected gold clusters may be used as promising building blocks with tunable energy gaps, tunneling barriers, and magnetic moments for applications in the area of electron and/or spin transport.

PACS numbers: 73.22.-f, 36.40.-c, 61.46.-w

Ligand monolayer protected gold clusters (MPCs) have received a lot of interest since mid-1990's due in part to their enhanced stability, easy synthesis, rather well-defined monodispersity and potential applications in nanotechnology. For example, the MPCs may be used as catalysts, sensors or building blocks for molecular electronic and spintronic devices [1–6]. They also form an interesting class of materials where the evolution of the clusters' electronic structure and "metallicity" from molecular to colloidal (bulk-like) regimes can be explored, e.g., by measuring the optical or electrochemical response with varying cluster sizes.

Recent refinements of the original synthesis[7] of MPCs by several groups have enabled monodisperse samples of a few particularly stable magic compounds in 1 - 3 nm range, and a few have by now been determined up to molecular precision; these include Au₂₀(SR)₁₆ [8], Au₂₅(SR)₁₈^{-1/0} [9–11], Au₃₈(SR)₂₄ [12, 13], Au₄₀(SR)₂₄ [14], Au₆₈(SR)₃₄ [15], Au₁₀₂(SR)₄₄ [16], and compounds around 144 Au atoms and 60 thiolates [12, 17, 18]. The Au₂₅, Au₃₈ and Au₁₀₂ clusters are notable in this series since their total atomic structure has been determined from X-ray crystallography, opening the door to detailed theoretical analysis of the surface-covalent gold-sulphur bond and the electronic and geometric factors underlying the stability of these specific compounds.

Up to now, these MPCs have been investigated as stand-alone entities computationally. However, understanding the interaction of MPCs with their environments is fundamentally important in order to assess their suitability as building blocks for components in applications in molecular electronics or spintronics. Here, we have embarked on these studies by studying computationally the interaction of the Au₂₅(SR)₁₈ cluster and

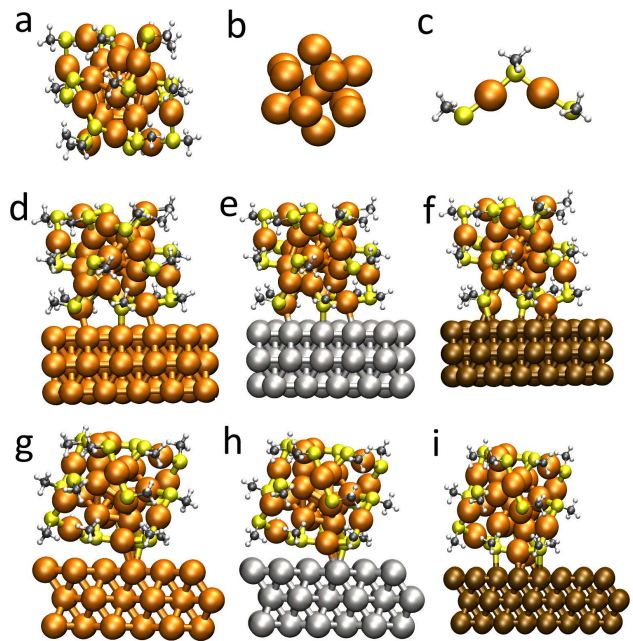


FIG. 1. The structure of (a) Au₂₅L₁₈⁻¹ cluster, (b) Au₁₃ core, (c) Au₂L₃ unit and Au₂₅L₁₈ cluster on (d) Au(111), (e) Ag(111) and (f) Cu(111) surface. (g), (h), (i) are the same structures as (d), (e), (f), but rotated 90 degrees. The atoms are colored as: Au: orange, S: yellow, C: dark grey, H: light grey, Ag: silver, Cu: brown.

its magnetically doped derivative MnAu₂₄(SR)₁₈ with a prototypical metal surface, for which we select the noble metal (111).

A particularly stable phenylethanethiolate-protected gold cluster, Au₂₅(SCH₂CH₂Ph)₁₈⁻¹ was structurally characterized from X-ray crystallography in 2008 [9, 10]

and its electronic and optical properties have been analyzed by using the density functional theory (DFT) [10, 19, 20]. The structure of the cluster is shown in Fig. 1a (from here on, we use methylthiolate SCH_3 as a model ligand and abbreviate $\text{L} = \text{SCH}_3$). It comprises an approximately icosahedral core of 13 Au atoms (see Fig. 1b) surrounded by six Au_2L_3 units (see Fig. 1c) in an octahedral arrangement with 12 S-Au contacts that passivate the core surface. The cluster $\text{Au}_{25}\text{L}_{18}^q$ is known to be a stable redox species with at least three possible charge (and spin) states: $q = -1, 0, +1$. This has led to suggestions that replacement of one or more core Au atoms by a magnetic atom such as Mn should lead to a "magnetic superatom"; theoretically this has been shown to be the case for an isolated $\text{MnAu}_{24}\text{L}_{18}$ [20, 21]. The robust geometry and a well-understood electronic and magnetic structure of these clusters motivated us to use $\text{Au}_{25}\text{L}_{18}$ and $\text{MnAu}_{24}\text{L}_{18}$ to investigate how metallic surfaces will affect the structure and properties of MPCs and whether the thiolate ligands can decouple the delocalized superatom orbitals and local spins from the electronic structure of the surface.

We use spin-polarized DFT as implemented in the GPAW code [22, 23]. The DFT calculations are performed with the projector-augmented-wave (PAW) method in a real space grid (0.2 Å grid spacing) using the Perdew-Burke-Ernzerhof (PBE) generalized-gradient approximation [24]. We regard $\text{Cu}(3d^{10}4s^1)$, $\text{Ag}(4d^{10}5s^1)$, $\text{Au}(5d^{10}6s^1)$, $\text{Mn}(3d^54s^2)$, $\text{S}(2s^22p^4)$, $\text{C}(2s^22p^2)$ and $\text{H}(1s^1)$ electrons as the valence. The PAW setups for all the metals include scalar-relativistic corrections. Periodic boundary conditions are applied in all the dimensions. The Au(111), Ag(111) and Cu(111) substrates are modeled with three layers and 15 Å vacuum is used to separate the Au_{25} cluster and the image slab in the z direction. The two bottom metallic layers are fixed but all other atoms are relaxed during the geometry optimization until forces are below 0.05 eV/Å. A (5x6) surface cell is constructed for Au(111) and Ag(111) surfaces while a (6x8) surface cell is constructed for Cu(111). A Monkhorst-Pack 2x2x1 k-point sampling and the Bader method [25] are used to analyze the electronic structure and the charge state of the cluster.

The relaxed structures of $\text{Au}_{25}\text{L}_{18}$ on Au(111), Ag(111) and Cu(111) surfaces are shown in Fig. 1d-1i. The geometrical structures of $\text{Au}_{25}\text{L}_{18}$ on Au(111) and Ag(111) surfaces are very similar. The shortest distance between the cluster and the surface atoms is 2.66 Å for the Au(111) surface and 2.69 Å for the Ag(111) surface which is the distance from one S atom to the Au (Ag) surface. Besides the S atom, there are two Au ligand atoms close to Au(111) and Ag(111) surfaces at 2.92 Å, 2.93 Å from the Au(111) surface and 2.93 Å, 2.98 Å from the Ag(111) surface. These three connections stabilize the cluster on the surface. Although some SCH_3 units are rotated by the interaction with the surfaces, the overall

	Cluster	Core	Ligands
$\text{Au}_{25}\text{L}_{18}^{-1}$	-1.00	0.31	-1.31
$\text{Au}_{25}\text{L}_{18}/\text{Au}(111)$	0.28	0.41	-0.13
$\text{Au}_{25}\text{L}_{18}/\text{Ag}(111)$	-0.42	0.34	-0.76
$\text{Au}_{25}\text{L}_{18}/\text{Cu}(111)$	-0.33	0.41	-0.74

TABLE I. The calculated charge decomposition (by the Bader method) of $\text{Au}_{25}\text{L}_{18}^{-1}$ and for the cluster on Au(111), Ag(111) and Cu(111). The core consists of the approximately icosahedral Au_{13} and the ligand layer consists of the six Au_2L_3 units.

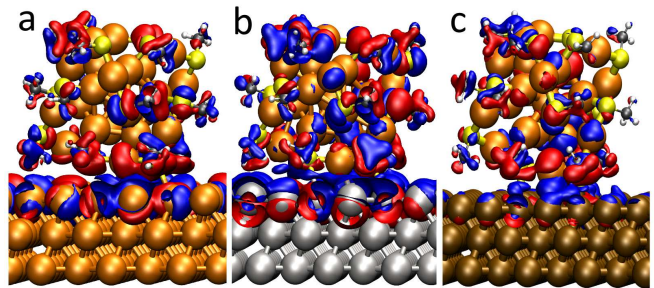


FIG. 2. The isosurface ($h=0.005\text{Å}^{-3}$) of $\delta\rho$ for $\text{Au}_{25}\text{L}_{18}$ on (a) Au(111), (b) Ag(111) and (c) Cu(111) surface. The blue and red regions show accumulated and depleted electron charge, respectively. The colors of atoms are as in Figure 1.

shape of the metal frame of the cluster remains spherical as in the case of $\text{Au}_{25}\text{L}_{18}^{-1}$ in the gas phase.

The structure of $\text{Au}_{25}\text{L}_{18}$ on Cu(111) is significantly different from Au(111) and Ag(111). The shortest distance between the cluster and the surface is also the distance between one S atom and Cu(111) surface (2.49 Å), but the symmetry of the cluster is severely broken. Two ligand Au atoms are displaced towards the surface: one stays approximately on the hollow position of the Cu(111) surface and another stays approximately on the bridge position. The shorter distance and the distortion of the cluster show that $\text{Au}_{25}\text{L}_{18}$ and Cu(111) surface have a strong interaction. This is reflected by the calculated adsorption energy ΔE of the cluster on the surface, for which we find values of -1.15 eV for Cu(111), -0.77 eV for Ag(111), and -0.53 eV for Au(111). It should be noted that our values are most likely slight underestimations of the true adsorption energies since the PBE functional does not include van der Waals -type (vdW) interactions. Anyway we expect that the above-mentioned systematic behavior is not changed by the neglected vdW effects.

When a MPC is placed on a metallic surface, the interactions between the MPC and the surface may induce the charge transfer effect which might change the electronic and magnetic properties of the cluster. In order to understand this effect, we calculated the Bader

charge distribution of the $\text{Au}_{25}\text{L}_{18}$ cluster on the different surfaces and compared it to the stable $\text{Au}_{25}\text{L}_{18}^{-1}$ in gas phase. The charge decomposition in the core and in the ligand layer of the cluster is given in Table I. 0.28 electrons are transferred from $\text{Au}_{25}\text{L}_{18}$ to the Au(111) surface, while 0.42 electrons are transferred from the Ag(111) surface to the cluster and 0.33 electrons are transferred from the Cu(111) surface to the cluster. We note that the charge transfer between the cluster and the surface shows the same trend as the work function (W) of the surface. The order of the work functions is $W(\text{Ag}(111)) < W(\text{Cu}(111)) < W(\text{Au}(111))$. If the Bader charges of the Au core and ligands are calculated separately, one can find out that the Au core has the similar charge state for $\text{Au}_{25}\text{L}_{18}^{-1}$ cluster and $\text{Au}_{25}\text{L}_{18}$ on the different surfaces, while the charge states of ligands are quite different, which indicates that the charge rearrangement of $\text{Au}_{25}\text{L}_{18}$ mainly happens in the ligand layer when the cluster adsorbs on the Au(111), Ag(111) and Cu(111) surfaces.

The real-space charge redistribution can be visualized by computing the quantity $\delta\rho = \rho_{clu+sub} - \rho_{clu} - \rho_{sub}$, where $\rho_{clu+sub}$ is the electron charge density for the combined system while ρ_{clu} and ρ_{sub} are the electron charge densities of the noninteracting cluster and substrate, respectively. The isosurface ($h=0.005\text{\AA}^{-3}$) of $\delta\rho$ for $\text{Au}_{25}\text{L}_{18}$ on Au(111), Ag(111) and Cu(111) is shown in Fig. 2. The blue region is where the electrons are accumulated and the red one is where the electrons are depleted. It is clear that the charge rearrangement is localized mainly in the ligands of the cluster and in the first layer of the metal surface. The different adsorption mechanism can also be seen in this figure. For $\text{Au}_{25}\text{L}_{18}/\text{Au}(111)$, the ligands which are close to the surface lose electrons, while the Au surface atoms which are close to ligands gain electrons. The coulomb interaction between the positive charge of the cluster and the negative charge of the surface makes the cluster stable on the surface. For $\text{Au}_{25}\text{L}_{18}/\text{Cu}(111)$, the electrons accumulate between the cluster and the surface which shows formation of a chemical-bond-like interaction between the cluster and the surface.

It is of great interest to analyze the electronic structure of the adsorbed cluster, especially the frontier orbitals near the Fermi level. The $\text{Au}_{25}\text{L}_{18}^{-1}$ has been studied previously [10, 19, 20]. The HOMO level is 3-fold degenerate whereas the LUMO is 2-fold degenerate with a HOMO-LUMO (HL) gap of about 1.3eV (PBE value). The character of the electronic states of the cluster can be analyzed by projection onto spherical harmonics placed at the mass center of the cluster [19, 26]:

$$c_{i,l}(R_0) = \sum_{m=-l}^l \int_0^{R_0} r^2 dr |\psi_{i,lm}(r)|^2, \quad (1)$$

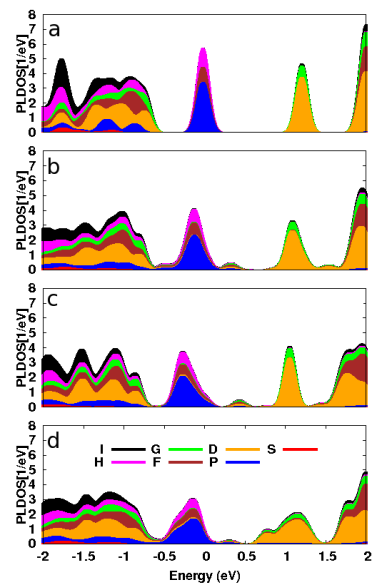


FIG. 3. The angular-momentum-projected local density of states (PLDOS) (projection up to I symmetry, i.e $l = 6$) for the Au_{13} core of (a) $\text{Au}_{25}\text{L}_{18}^{-1}$, (b) $\text{Au}_{25}\text{L}_{18}$ on Au(111), (c) $\text{Au}_{25}\text{L}_{18}$ on Ag(111), and (d) $\text{Au}_{25}\text{L}_{18}$ on Cu(111). The individual weights $c_{i,l}$ have been folded by a Gaussian of 0.1 eV width. The Fermi energy is at zero.

where

$$\psi_{i,lm}(r) = \int d\hat{r} Y_{lm}(\hat{r}) \phi_i(r), \quad (2)$$

Here i is the index of the Kohn-Sham state $\phi(r)$ and Y_{lm} is the spherical harmonic function with l as the angular quantum number and m as the magnetic quantum number. The angular momenta are considered up to $l = 6$ (I-symmetry) and the expansion is made in a sphere of radius R_0 , where R_0 is chosen to be 4.5 \AA . This analysis reveals the symmetry of the Kohn-Sham states of the system in the Au_{13} core. Previously this analysis showed for $\text{Au}_{25}\text{L}_{18}^{-1}$ that the HOMO has P-symmetry and the LUMO has D-symmetry as shown in Fig. 3a. This result is easy to understand from the superatom model: The "free-electron" count for $\text{Au}_{25}\text{L}_{18}^{-1}$ is defined by the 26 Au(6s) electrons (including the extra electron from the negative charge) "donated" to the sp-subsystem, out of which 18 electrons are withdrawn by the thiolates, resulting in eight delocalized electrons with closed electronic shell at $1\text{S}^21\text{P}^6$. [19, 26]

Here we extend the use of eqs. 1 and 2 to analyze the electronic shells of the metal core of the adsorbed clusters. The angular-momentum-projected local electron density of states (PLDOS) for the $\text{Au}_{25}\text{L}_{18}$ on the Au(111), Ag(111) and Cu(111) are shown in Fig. 3b-3d respectively. Neglecting the very small feature just above the Fermi level (originating from the interaction between the cluster and the surface), the HOMO of the cluster in all cases has a clear P-symmetry and the LUMO has a

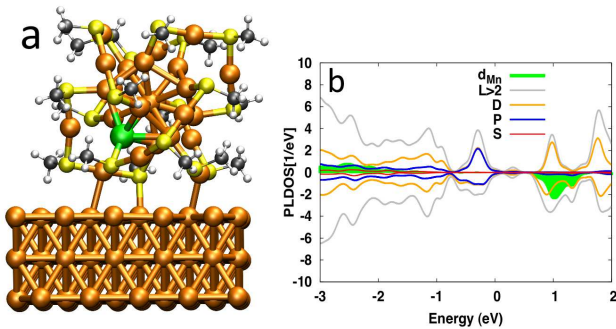


FIG. 4. (a) The structure of $\text{MnAu}_{24}\text{L}_{18}$ on $\text{Au}(111)$. Mn is green, the other colors as in Figure 1. (b) The angular-momentum-projected local density of states (PLDOS) of the MnAu_{12} core ($R_0 = 4.5\text{\AA}$ in eq. 1) and Mn atom ($R_0 = 1.4\text{\AA}$ in eq. 1) of $\text{MnAu}_{24}\text{L}_{18}$ on $\text{Au}(111)$. Top and bottom panels show the PLDOS for spin up and down electrons, respectively. The individual weights $c_{i,l}$ have been folded by a Gaussian of 0.1 eV width. The Fermi energy is at zero.

clear D-symmetry. This shows that the "superatomic orbitals" exist also when the cluster is adsorbed on the metal surfaces. From the peak positions, the apparent "HL gaps" for the clusters can be determined. For the $\text{Au}(111)$ and $\text{Ag}(111)$ surfaces, the HL gap is about 1.0 eV, slightly reduced from the gas phase value of the $\text{Au}_{25}\text{L}_{18}^{-1}$ cluster. The HL gap further diminishes when the cluster is on the $\text{Cu}(111)$ surface (0.7eV), mainly because the LUMO states broaden into a wider band, caused by the stronger interaction between the cluster and Cu surface.

If a cluster retains a magnetic moment on the surface, it may have possible applications for spin-dependent transport in molecular spintronics. The neutral $\text{Au}_{25}\text{L}_{18}$ has a magnetic moment $1\mu_B$ in the gas phase, but we found that the moment is quenched on all the (111) surfaces. The Mn-doped $\text{MnAu}_{24}\text{L}_{18}$ has a high moment of $5\mu_B$ in gas phase due to the localized $\text{Mn}(3d^5)$ electrons.[20, 21] We found that the energetically optimal site of the Mn atom is in the surface of the Au_{13} core, in agreement with another recent DFT study[27]. The energy differences to the next structure isomers are 0.30 eV and 0.36 eV (corresponding to Mn in the ligand layer and at the center of the core, respectively). Motivated by this result we replaced one of the Au_{13} core surface atoms, facing $\text{Au}(111)$, by the Mn atom. We find that the structure of the doped $\text{MnAu}_{24}\text{L}_{18}/\text{Au}(111)$ and $\text{Au}_{25}\text{L}_{18}/\text{Au}(111)$ are very similar (see fig. 4a). However in contrast to the $\text{Au}_{25}\text{L}_{18}/\text{Au}(111)$ case, we observe that the magnetic moment of $\text{MnAu}_{24}\text{L}_{18}/\text{Au}(111)$ remains very high, $4.9\mu_B$, with $4.6\mu_B$ localized on the Mn atom. We show the PLDOS of the MnAu_{12} core and the Mn atom of $\text{MnAu}_{24}\text{L}_{18}/\text{Au}(111)$ in Fig. 4b. The 3d orbitals of the Mn atom remain fully spin-polarized which gives rise to the high magnetic moment of the cluster.

Simultaneously, the frontier orbitals of the cluster retain the P symmetry for HOMO and D symmetry for LUMO.

In conclusion, using methylthiolate protected $\text{Au}_{25}\text{L}_{18}$ and a doped $\text{MnAu}_{24}\text{L}_{18}$ as prototype clusters, we studied the interaction between MPCs and noble metal (111) surfaces. The geometric structure of the cluster and the adsorption mechanism depend on the interaction between the ligands and the surface, but the structure and the electronic properties of the core remain. The charge rearrangement is localized in the ligand layer which protects the overall electronic shell structure of both $\text{Au}_{25}\text{L}_{18}$ and $\text{MnAu}_{24}\text{L}_{18}$ and localized spins of Mn 3d electrons in the core of $\text{MnAu}_{24}\text{L}_{18}$ by decoupling them from the surface. The HOMO-LUMO gap of the adsorbed cluster depends slightly on the metal, being the smallest on the $\text{Cu}(111)$ which also has the strongest interaction with the cluster. However a clear gap of about 0.7 eV to 1 eV is observed in all cases. Our results implicate that monodispersed thiolate-protected gold clusters retain their "superatom identity" also when adsorbed on prototypical metal surfaces. These novel building blocks can be experimentally synthesized in pure forms, can be doped by magnetic atoms, and their ligand layer can be functionalized by varying the nature (e.g., aryl- or alkylthiolates) and size of the ligands which affects the electronic coupling and tunneling barriers. Utilizing this diversity may open new ways to engineer building blocks for molecular electronic and spintronic devices.

This research is supported by the Academy of Finland (FiDiPro project) and CSC - the Finnish IT Center for Science. X.C. wishes to thank O. Lopez-Acevedo and P.A. Clayborne for help with GPAW.

*Present address: Center for Atomic-scale Materials Design, Department of Physics, Technical University of Denmark, DK-2800 Kgs. Lyngby, Denmark.

**Corresponding author: hakkinen.hannu@gmail.com

-
- [1] A. C. Templeton, W. P. Wuefling, and R. W. Murray, *Acc. Chem. Res.*, **33**, 27 (2000).
 - [2] M. C. Daniel and D. Astruc, *Chem. Rev.*, **104**, 293 (2004).
 - [3] H. Häkkinen, *Chem. Soc. Rev.*, **37**, 1847 (2008).
 - [4] R. Sardar, A. M. Funston, P. Mulvaney, and R. W. Murray, *Langmuir*, **25**, 13840 (2009).
 - [5] R. C. Jin, *Nanoscale*, **2**, 343 (2010).
 - [6] O. Lopez-Acevedo, K. A. Kacprzak, J. Akola, and H. Häkkinen, *Nature Chemistry*, **2**, 329 (2010).
 - [7] M. Brust, M. Walker, D. Bethell, D. J. Schiffrin, and R. Whyman, *Chem. Comm.*, **1994**, 801 (1994).
 - [8] M. Z. Zhu, H. F. Qian, and R. C. Jin, *J. Am. Chem. Soc.*, **131**, 7220 (2009).
 - [9] M. W. Heaven, A. Dass, P. S. White, K. M. Holt, and R. W. Murray, *J. Am. Chem. Soc.*, **130**, 3754 (2008).
 - [10] M. Zhu, C. M. Aikens, F. J. Hollander, G. C. Schatz, and R. Jin, *J. Am. Chem. Soc.*, **130**, 5883 (2008).

- [11] M. Zhu, W. T. Eckenhoff, T. Pintauer, and R. C. Jin, *J. Phys. Chem. C*, **112**, 14221 (2008).
- [12] N. K. Chaki, Y. Negishi, H. Tsunoyama, Y. Shichibu, and T. Tsukuda, *J. Am. Chem. Soc.*, **130**, 8608 (2008).
- [13] H. F. Qian, W. T. Eckenhoff, Y. Zhu, T. Pintauer, and R. C. Jin, *J. Am. Chem. Soc.*, **132**, 8280 (2010).
- [14] H. F. Qian, Y. Chu, and R. C. Jin, *J. Am. Chem. Soc.*, **132**, 4583 (2010).
- [15] A. Dass, *J. Am. Chem. Soc.*, **131**, 11666 (2009).
- [16] P. D. Jadzinsky, G. Calero, C. J. Ackerson, D. A. Bushnell, and R. D. Kornberg, *Science*, **318**, 430 (2007).
- [17] H. F. Qian and R. C. Jin, *Nano Lett.*, **9**, 4083 (2009).
- [18] C. A. Fields-Zinna, R. Sardar, C. A. Beasley, and R. W. Murray, *J. Am. Chem. Soc.*, **131**, 16266 (2009).
- [19] J. Akola, M. Walter, R. L. Whetten, H. Häkkinen, and H. Grönbeck, *J. Am. Chem. Soc.*, **130**, 3756 (2008).
- [20] J. Akola, K. A. Kacprzak, O. Lopez-Acevedo, M. Walter, H. Grönbeck, and H. Häkkinen, *J. Phys. Chem. C*, **114**, 15986 (2010).
- [21] J. U. Reveles, P. A. Clayborne, A. C. Reber, S. N. Khanna, K. Pradhan, P. Sen, and M. R. Pederson, *Nature Chemistry*, **1**, 310 (2009).
- [22] J. J. Mortensen, L. B. Hansen, and K. W. Jacobsen, *Phys. Rev. B*, **71**, 035109 (2005).
- [23] J. Enkovaara and et al, *J. Phys. Condens. Matter*, **22**, 253202 (2010).
- [24] J. P. Perdew, K. Burke, and M. Ernzerhof, *Phys. Rev. Lett.*, **77**, 3865 (1996).
- [25] W. Tang, E. Sanville, and G. Henkelman, *J. Phys. Condens. Matter*, **21**, 084204 (2009).
- [26] M. Walter, J. Akola, O. Lopez-Acevedo, P. D. Jadzinsky, G. Calero, C. J. Ackerson, R. L. Whetten, H. Grönbeck, and H. Häkkinen, *Proc. Natl. Acad. Sci (USA)*, **105**, 9157 (2008).
- [27] M. Zhou, Y. Q. Cai, M. G. Zeng, C. Zhang, and Y. P. Feng, *Appl. Phys. Lett.*, **98**, 143103 (2011).